Article

pubs.acs.org/Biomac

Effect of 3D Matrix Compositions on the Efficacy of EGFR Inhibition in Pancreatic Ductal Adenocarcinoma Cells

Chang Seok Ki, Han Shih, and Chien-Chi Lin*

Department of Biomedical Engineering, Purdue School of Engineering and Technology, Indiana University-Purdue University at Indianapolis, Indianapolis, Indiana 46202, United States

Supporting Information

ABSTRACT: Therapeutics to inhibit signaling of epidermal growth factor receptor (EGFR) has been suggested as a potential treatment for pancreatic cancers, and two-dimensional (2D) cell culture techniques are commonly used to identify and/or verify the therapeutic efficacy of EGFR inhibitors. However, drug targets identified from conventional cell culture techniques may not exhibit desired functions when these drugs are tested in animal studies, in large part due to the complicated tumor microenvironments. Hence, it is crucial to develop a biomimetic cell culture system capable of recapitulating aspects of tumor niches for studying cancer cell fate processes under the influence of various environmental stimuli. In this study, we utilized a versatile PEG-peptide hydrogel system to demonstrate the influence of matrix properties and EGFR inhibition on the growth of a pancreatic ductal adenocarcinoma cell line (PANC-1). PANC-1 cells were encapsulated in 8-arm PEG-norbornene (PEG8NB) hydrogels cross-linked by matrix metalloproteinase (MMP) sensitive peptide (MMP_{Linker}) using thiol−ene photoclick chemistry. In soft hydrogels ($G' \sim 2$ kPa), cells retained high initial viability and formed clusters after prolonged culture, whereas cells encapsulated in stiff hydrogels ($G' \sim 12$ kPa) exhibited lower initial viability and reduced proliferation. While the immobilization of an EGFR peptide inhibitor, Asn-Tyr-Gln-Gln-Asn or NYQQN, in soft hydrogels did not cause cell death, this peptide induced significant cell apoptosis when immobilized in stiff hydrogels. Western blotting results showed that cell death was due to reduced expression of EGFR and Akt in stiff hydrogels under the influence of immobilized NYQQN peptide. These results shed light on the importance and non-negligible role of matrix properties on the efficacy of antitumor drugs.

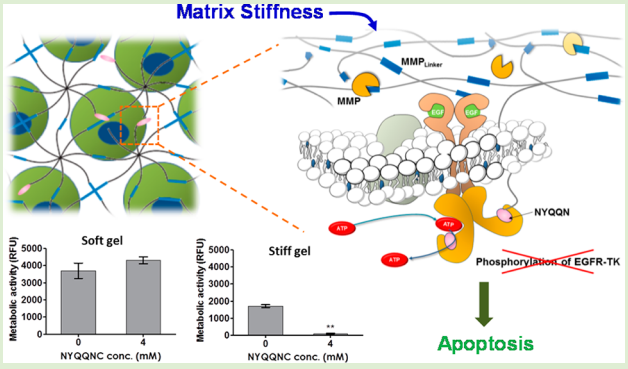

INTRODUCTION

Pancreatic cancers are the fourth leading cause of all cancer-related deaths. In most cases, pancreatic cancers are diagnosed in the late stages with poor prognosis. Clinical options for tumor treatments, such as chemotherapy, are less effective in pancreatic cancers due to high resistance of pancreatic tumor cells to anticancer drugs. Moreover, pancreatic cancers show aggressive metastasis and have very low survival rate. Following diagnosis, it is estimated that patients on average live for only 6 months and 5-year survival rate is less than 6%.[1−3] Pancreatic ductal adenocarcinoma (PDAC) accounts for more than 90% of all forms of pancreatic cancers. The development of PDAC is a complicated process involving high frequency of gene mutations, property changes in the local tissue microenvironment, as well as abnormal expression of many growth factors and their receptors, including vascular endothelial growth factor (VEGF), fibroblast growth factor-2 (FGF-2), transforming growth factor β1 (TGF-β1), and epidermal growth factor (EGF). Together, these factors contribute to epithelial-to-mesenchymal transition (EMT) that is believed to cause tumor metastasis.[3−5]

Studies have shown that the growth and metastasis of PDAC are highly relevant to the overexpression of EGF receptor (EGFR) in PDAC cells.[1,6] EGFR is a tyrosine kinase (TK) receptor that transduces signals upon binding to EGF. EGFR modulates diverse cellular activities, such as proliferation, survival, and differentiation. Moreover, it is closely related to the progression and metastasis of various epithelial tumors, including nonsmall cell lung cancer, breast cancer, and PDAC.[4,7−9] EGFR has been suggested as a therapeutic target for suppressing the proliferation and metastasis of cancer cells.[5,10−13] For example, monoclonal antibodies (mAb), such as cetuximab (C225), have been used to block the ligand-binding region of EGFR, thus inhibiting its activation.[14] In addition, many small molecule inhibitors (e.g., erlotinib, gefitinib, lapatinib) are used to competitively bind to the adenosine triphosphate (ATP) binding site in EGFR, thus preventing receptor phosphorylation.[15−17] Alternatively, peptide drugs can be used to inhibit tumor growth.[18−20] Peptide-

Received: March 30, 2013
Revised: July 26, 2013
Published: July 27, 2013

 © 2013 American Chemical Society

based drugs are more stable than mAb and can be easily synthesized in a large quantity via standard peptide synthesis procedures. Furthermore, the amino acid sequences of peptide drugs can be easily modified for diverse applications and/or for improving therapeutic efficacy. Based on a structural docking simulation, Abe et al. have identified a 5-mer peptide, Asn-Tyr-Gln-Gln-Asn (NYQQN), that inhibits phosphorylation of soluble EGFR. In an ATP-independent manner, NYQQN binds to a hydrophobic region next to the ATP binding pocket of EGFR-TK, resulting in the blockage of catalytic site essential for EGFR phosphorylation.[10] This peptide drug, however, has not been tested in pancreatic cancer cells.

The effects of receptor inhibitors are commonly tested on two-dimensional (2D) surfaces, such as tissue culture plastic (TCP), followed by in vivo studies using animal models. While 2D culture platforms have facilitated the discovery of key factors affecting tumor cell growth, it is also increasingly recognized that cell fate processes are tightly regulated by a myriad of extracellular cues presented in a three-dimensional (3D) manner.[21,22] For example, recent reports have shown that matrix stiffness dictates intracellular mechanosensing, which affects cell adhesion, proliferation, migration, differentiation, and apoptosis in 3D.[23−25] Tumor metastasis is also closely related to the stiffness of a tumor tissue.[23,26,27] However, correlations between matrix properties, EGFR activation, and tumor cell fate in 3D have not been extensively studied, perhaps due to the lack of an appropriate material platform. Recent efforts on 2D cell culture have started to shed light on the role of matrix stiffness on EGFR activation in epithelium cells. For example, Kim and Asthagiri reported that stiff acrylamide gel surface increased EGFR sensitivity in Madin-Darby canine kidney (MDCK) cells and attenuated contact inhibition of proliferation.[28]

Environmental cues and stimuli with known effects on tumor cells in 2D culture may not elicit the same cellular responses when the cells were cultured in a 3D matrix.[29] Commercially available 3D culture matrices, such as Matrigel, often contain undefined matrix components and residual growth factors, and have poor mechanical properties that may not be ideal to recapitulate a complex and often stiffen tumor microenvironment. Hence, there is a need to develop biomimetic and adaptable matrices for evaluating tumor cell fate process in 3D and for testing the therapeutic efficacy of antitumor drugs.[5,30] To this end, a wide variety of synthetic materials have been explored as 3D matrices to mimic extracellular matrix (ECM) microenvironment.[31−34] Poly(ethylene glycol) (PEG) hydrogels are among the most commonly used synthetic materials for 3D cell culture because of their high water content, tissue-like elasticity, and tunable biophysical and biochemical properties.[35] By manipulating polymer network cross-linking density, the stiffness of the gel matrix can be easily controlled to mimic tissues with certain mechanical property. Cell−ECM interactions can also be engineered by incorporating cell-responsive motifs within the otherwise inert PEG hydrogels. Classic examples include the use of integrin ligand RGD peptide to promote cell attachment[36,37] and the use of matrix metalloproteinase (MMP) sensitive peptides as part of the hydrogel network to permit cell-mediated matrix remodeling.[38]

PEG-based hydrogels have been used as 3D matrices for some tumor cell studies.[39−43] However, limited efforts have been devoted to using PEG-based hydrogels for understanding pancreatic cancer cell behaviors. In this contribution, we employed biomimetic and highly tunable PEG-peptide hydrogels with exquisite control over material properties[44,45] for studying the effect of EGFR inhibition on pancreatic tumor cell behaviors in 3D. Specifically, thiol−ene photoclick chemistry was utilized to fabricate PEG-peptide hydrogels with a wide range of moduli, protease sensitivity, and peptide inhibitory effect. Stiffness of the hydrogel matrix was controlled by adjusting the degree of polymer cross-linking. Protease sensitivity of the gel matrix was tuned by using dithiothreitol (DTT) or MMP-sensitive peptide (KCGPQG↓IWGQCK, arrow indicates enzyme cleavage site) as the gel cross-linker. Finally, receptor inhibition in the encapsulated pancreatic ductal adenocarcinoma (PANC-1) cells was induced by the immobilization of a known EGFR peptide inhibitor (NYQQNC, cysteine residue added for immobilization in the thiol−ene network). This material platform was used as a model system to illustrate the influences of matrix properties on EGFR inhibition, which were evaluated by characterizing cell metabolic activity, morphology, apoptosis, and EGFR-related protein expression.

MATERIALS AND METHODS

Materials. 8-Arm poly(ethylene glycol) (20 kDa) was purchased from JenKem Technology USA. Fmoc-amino acids, Fmoc-Rink-amide MBHA resin, and peptide synthesis reagents were acquired from Anaspec or Chempep, Inc. 3-(4,5-Dimethylthiazol-2-yl)2,5-diphenyltetrazolium (MTT) and AlamarBlue reagents were purchased from Fisher Scientific and AbD Serotec, respectively. Live/dead staining kit for mammalian cells and DAPI stain were obtained from Invitrogen. Caspase-Glo 3/7 assay kit and CaspACE FITC-VAD-FMK in situ marker were purchased from Promega. EFG receptor XP rabbit mAb, Akt rabbit mAb, anti-rabbit IgG, and anti-mouse IgG HRP-linked antibodies were obtained from Cell Signaling Technology. HPLC grade acetonitrile and water were acquired from Fisher Scientific and VWR International, respectively. All other chemicals were purchased from Sigma-Aldrich unless noted otherwise.

8-Arm PEG-Norbornene and Lithium Arylphosphinate Synthesis. PEG-octa-norbornene (PEG8NB) was synthesized according to an established protocol.[46] Briefly, 8-arm PEG-OH was dried in a vacuum oven overnight and dissolved in anhydrous toluene. After removing toluene with a rotary evaporator, the dried PEG was dissolved in anhydrous dichloromethane (DCM). In a separate flask, 5-norbornene-2-carboxylic acid (5 equiv to OH group on PEG) was reacted with *N*,*N*′-dicyclohexlycarbodiimide (DCC, 2.5 equiv) in anhydrous DCM for at least 15 min at room temperature to form norbornene anhydride. Subsequently, the solution was filtered through a fritted funnel and added drop-wise into the flask (placed in an ice bath) containing dried 8-arm PEG-OH, 4-(dimethylamino)pyridine (DMAP, 0.5 equiv), and pyridine (5 equiv) in DCM. All reactions were performed under nitrogen. After overnight reaction, the product (PEG8NB) was filtered, washed with 5 wt % sodium bicarbonate and brine to remove unreacted norbornene acid, and residual water was removed by sodium sulfate. The product was then filtered and precipitated in cold ethyl ether (repeated twice). Purified PEG8NB was dried in a vacuum desiccator, and the degree of functionalization (80−90%) was determined using ^{1}H NMR (Avance III 500, Bruker). The photoinitiator lithium arylphosphinate (LAP) was synthesized according to a published protocol without modification.[46]

Peptide Synthesis. All peptides, KCGPQGIWGQCK (MMP_{Linker}),[47,48] NYQQN, and NYQQNC, were synthesized using Fmoc-Rink-Amide HBMA resin in a microwave-assisted solid peptide synthesizer (CEM Discover SPS) following standard HOBT/HBTU coupling chemistry. Deprotection of Fmoc groups and coupling of Fmoc-amino acids (with the exception of Fmoc-Cys(Trt)-OH) were performed at 50 W, 75 °C for 3 and 5 min, respectively. Coupling of Fmoc-Cys(Trt)-OH was performed at 50 W, 50 °C for 10 min to reduce racemization. The peptides were also cleaved in the microwave peptide synthesizer (38 °C, 20 W, 30 min) using a cleavage cocktail

containing 95% trifluoroacetic acid (TFA), 2.5% water, and 2.5% triisopropylsilane (TIS) in the presence of 5% (w/v) phenol. Crude peptides were precipitated in cold ethyl ether, dried overnight in a desiccator, purified using HPLC (PerkinElmer Flexar System), and characterized by mass spectrometry (Agilent Technologies). Purified peptides were lyophilized and stored in −20 °C. The concentration of thiol groups on purified cysteine-containing peptides was quantified using Ellman's reagent (PIERCE).

Cell Culture and Encapsulation. PANC-1 cells (from ATCC) were maintained in high glucose DMEM (HyClone) containing 10% fetal bovine serum (Gibco) and 1× Antibiotic-Antimycotic (Invitrogen, 100 U/mL penicillin, 100 μg/mL streptomycin, and 250 ng/mL Fungizone). Cells were cultured in tissue culture Petri-dishes kept at 37 °C and 5% CO_2, and the medium was changed every 2 or 3 days. Prior to cell encapsulation, prepolymer solutions containing PEG8NB, dithiol cross-linker (MMP_{Linker} or DTT), EGFR inhibitor (0−4 mM NYQQNC), and 1 mM LAP were prepared. Table S1 in the Supporting Information lists the compositions of all hydrogel formulations used in this study. Each gel formulation contained an additional 4 mM norbornene group that was available for the incorporation of up to 4 mM NYQQN peptide.

For cell encapsulation, trypsinized PANC-1 cells were suspended in a prepolymer solution at a desired cell density (2×10^6 or 5×10^6 cells/mL). Twenty-five microliters of prepolymer solution was placed in a 1 mL disposable syringe with a cut-open tip and exposed to UV light (365 nm, 5 mW/cm^2) for 2 min (Figure 1A). After photopolymerization, cell-laden hydrogels were maintained in identical cell culture conditions as described earlier.

Characterization of Hydrogel Modulus, Cross-Linking Density, and Peptide Incorporation Efficiency. Shear moduli of the hydrogels were measured on a digital rheometer (Bohlin CVO 100). To prepare cell-laden hydrogels, prepolymer solution (PEG8NB-MMP_{Linker} or -DTT) containing 1 mM of photoinitiator LAP and PANC-1 cells (at 5×10^6 cells/mL) was injected between two glass slides separated by 1 mm thick spacers. Gels were formed by photopolymerization (365 nm, 5 mW/cm^2) for 2 min. Circular discs were punched out from the hydrogel slab using a biopsy punch (diameter 8 mm) and incubated in cell culture medium at 37 °C and 5% CO_2. The shear moduli of the cell-laden hydrogels were measured at day-0 (immediately following gelation) and day-10 postencapsulation. Gels without cells were prepared and characterized with the same methods. Strain sweep (0.1−20%) oscillatory rheometry was performed using a parallel plate geometry (8 mm) with a gap size of 800 μm. Shear moduli (G') in the linear viscoelastic region (LVR) were reported and used to calculate the cross-linking density (ρ) of the gels using the following equation:[49]

$$\rho\ (\mathrm{mM}) = \frac{G' M_S}{RT} \quad (1)$$

where G' is shear modulus, M_s is average molecular weight between cross-links, R is the gas constant, and T is the temperature.

The efficiency of pendant peptide immobilization was characterized as described below. Prepolymer solutions containing 4 mM NYQQNC peptide and various PEG8NB concentrations (i.e., 4, 6, and 8 wt %, prepared as described earlier) were photo-cross-linked as described above. Following polymerization, each 25 μL gel was incubated in 400 μL of distilled water for 24 h to remove soluble fractions containing peptides that were not immobilized in the network. Next, collected solutions were characterized by analytical RP-HPLC. The concentrations of released peptide were calculated by using HPLC traces with known peptide concentrations and used to calculate peptide immobilization efficiency.

Cell Viability Assays. To measure cell viability under the influence of EGFR inhibitor (NYQQN) in 2D culture, PANC-1 cells were seeded in a 96-well tissue culture plate (5000 cells/well) and cultured until 80% confluence. The cells were treated with NYQQN for 1−3 days, followed by MTT assay (0.05% MTT in fresh culture medium). After 4 h incubation at 37 °C and 5% CO_2, purple formazan crystal was dissolved using DMSO. The optical absorbance of the solution was measured at 540 nm using a microplate reader (BioTek Synergy HT). To measure encapsulated cell metabolic activity, cell-laden hydrogels were incubated in 500 μL of 10% AlamarBlue reagent in culture medium for 2 h (for 5×10^6 cells/mL) to 4 h (for 2×10^6 cells/mL). Following incubation, 200 μL of the culture media was transferred to a 96-well plate and fluorescence generated due to nonspecific cellular metabolic activity was measured using a microplate reader (excitation, 560 nm; emission, 590 nm). Qualitative cell viability following photoencapsulation was characterized by live/dead staining and confocal imaging. Cell-laden hydrogels were incubated in live/dead staining solution for 1 h at room temperature with gentle shaking. Confocal images of the stained samples were obtained using an Olympus Fluoview FV100 laser scanning biological microscope. Z-Stack images (100 μm thick, 10 μm per slice) of at least four random fields were acquired. The ratio of live/dead cell counts was used to represent cell viability. To assess cell proliferation in PEG8NB-MMP_{Linker} hydrogel, DNA contents of the encapsulated cells were measured at day-1 and day-10 postencapsulation. Hydrogels were homogenized using a pellet mixer and digested in 1 mg/mL papain solution at 56 °C for 2 h. Subsequently, total DNA was isolated from digested gel and cell mixture using DNeasy Blood & Tissue kit (Qiagen) and quantified by QuantiFluor dsDNA assay kit (Promega).

Caspase Activity Assay. PANC-1 cells at 5×10^6 cells/mL were encapsulated in hydrogels with or without 4 mM NYQQNC immobilization. Cell metabolic activity was first determined by AlamarBlue assay 2 h after the encapsulation (day-0) as described earlier. Cell-laden hydrogels were subsequently incubated in fresh culture medium for 2 h and washed with PBS twice to remove residual AlamarBlue reagent, followed by incubation in Caspase-Glo 3/7 reagent solution (Promega) in the dark at room temperature for 1 h. The solution luminescence was measured by a microplate reader and normalized by the metabolic activity (determined by the AlamarBlue assay) in the respective samples. Activated caspases in PANC-1 cells

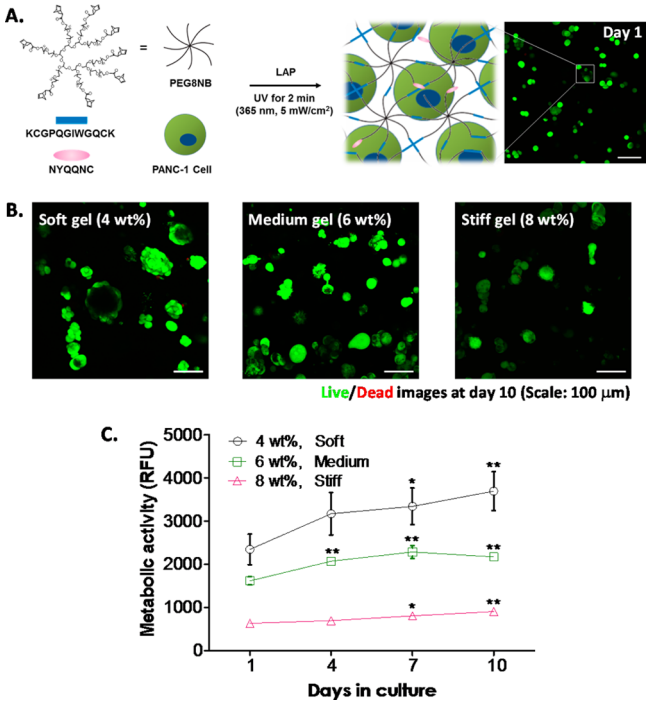

Figure 1. (A) Schematics of thiol−ene reaction to form PEG-peptide hydrogels for 3D culture of PANC-1 cells (not to scale) and a representative day-1 PANC-1 cell live (green)/dead (red) staining image (2×10^6 cells/mL). (B) Representative PANC-1 live/dead images at day-10. Cells were encapsulated in gels with different stiffness (soft gel, 1.9 kPa; medium gel, 6.7 kPa; and stiff gel, 11.8 kPa). (C) Metabolic activity of PANC-1 cells encapsulated in hydrogels prepared from 4, 6, or 8 wt % PEG8NB and MMP_{Linker} ($n = 3$, $^*p < 0.05$, $^{**}p < 0.01$, compared to day-1 in each group).

dx.doi.org/10.1021/bm4004496 | Biomacromolecules 2013, 14, 3017−3026

were also stained with CaspACE FITC-VAD-FMK (Promega). Cell nuclei were counter-stained with DAPI and images were acquired by a confocal microscope.

Western Blotting. Total protein from the encapsulated cells was extracted by homogenizing cell-laden hydrogels using a pellet mixer and lysed with RIPA buffer containing halt protease inhibitor (10 μL/mL), EDTA (5 mM) and 20 μM of phenylmethylsulfonyl fluoride (PMSF). Total protein extract was cleared by centrifugation at 8000 rpm for 10 min at 4 °C and concentrated using a centrifugal filter unit (Amicon Ultra, Millipore) at 14 000 rpm for 20 min at 4 °C. Total protein concentration was determined by BCA protein quantification kit (Pierce), separated by SDS-PAGE, and transferred to 0.45 μm Immobilon-P PVDF transfer membrane (Millipore) using a Trans-Blot Turbo Transfer System (BioRad). The blots were blocked overnight with 5% nonfat milk in TBST solution (PBS containing 0.05% Tween 20) at 4 °C, followed by incubation in primary antibody (rabbit anti-EGFR 1:900, rabbit anti-Akt 1:900, or mouse anti-β-actin 1:600) and HRP-conjugated secondary antibody (1:800) for 1 h each at room temperature. The blots were washed with TBST solution for 1 h and treated with a chemiluminescence detection kit (SuperSignal West Pico Detection Kit, Thermo Scientific). Immunoblotting images were obtained using a chemiluminescence imaging system (LAS3000, Fuji Film), and the intensities of the protein bands were analyzed using NIH ImageJ software.

Statistics. All experiments were conducted independently for three times, and the results were presented as mean ± SD. Each condition or gel formulation used in each experiment contained at least three gel samples. Statistical significance was determined using two-way ANOVA test. Difference was considered statistically significant when $p < 0.05$.

RESULTS

PEG-Peptide Hydrogels for PANC-1 Cell Encapsulation. Figure 1A outlines the procedures of PANC-1 cell encapsulation in thiol−ene hydrogels photocross-linked by PEG8NB and matrix metalloproteinase (MMP) sensitive peptide linker (MMP_{Linker}: KCGPQG↓IWGQCK). PANC-1 cells (2×10^6 cells/mL) encapsulated in 4 wt % PEG-MMP_{Linker} hydrogels retained high viability (92% live cell) 1-day postencapsulation. After 10 days, cells formed larger clusters with some hollow cystlike structures in softer gels, while more compact clusters formed in stiffer gels (Figure 1B). High degree of cell proliferation in soft hydrogel was also supported by an increase amount of total DNA recovered from cell-laden hydrogels (from ∼160 ng/gel in day-1 to ∼220 ng/gel in day-10, Figure S1, Supporting Information). Figure 1C shows the metabolic activity of encapsulated PANC-1 cells in hydrogels prepared with three PEG8NB concentrations (4, 6, and 8 wt %, representing hydrogels with soft, medium, and stiff modulus, Table S2, Supporting Information). In soft gels, cells exhibited higher initial metabolic activity, whereas cells encapsulated in stiffer hydrogels had lower initial metabolic activity (∼20−65% compared to metabolic activity in 4 wt % gels, Figure 1C). After 10-day culture in hydrogels, however, cell metabolic activity increased significantly in all three gel formulations with different stiffness.

Effect of EGFR Peptide Inhibitor on PANC-1 Cell Viability in 3D: Influence of Matrix Stiffness. The effect of immobilized NYQQNC peptide depended largely on the stiffness of the gels (Figure 2). For example, the immobilization of 4 mM peptide did not decrease cell metabolic activity in soft gels but caused significant cell death in stiff hydrogels. Controlled experiments showed that the differences in cell viability were not due to variation in immobilized peptide concentration because high peptide incorporation efficiencies (88−93%) were obtained in all three gel cross-linking densities

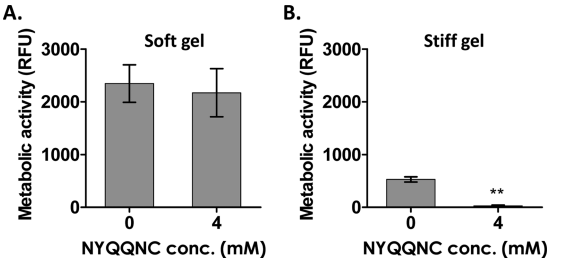

Figure 2. Effect of EGFR peptide inhibitor (NYQQNC) on the metabolic activity of PANC-1 cells (2×10^6 cells/mL) encapsulated in PEG-MMP_{Linker} hydrogels with (A) 4 wt % and (B) 8 wt % PEG8NB. Metabolic activity was measured at day 1 ($n = 3$, $^{**}p < 0.01$).

(Figure S2, Supporting Information). The immobilized peptide also did not significantly affect hydrogel stiffness after gel cross-linking, although slight degreases in the stiffness of medium and stiff gels immobilized with 4 mM peptide were obtained after 10 days (Table S2, Supporting Information). Additional control experiments show that PANC-1 cells remained viable in 2D culture even in the presence of 8 mM soluble NYQQN peptide (Figure S3, Supporting Information). Note that this peptide was previously used at 4 mM to inhibit phosphorylation of soluble EGFR.[10]

Effect of EGFR Peptide Inhibitor on PANC-1 Cell Viability in 3D: Influence of Cell-Mediated Matrix Remodeling. Figure 3 shows the importance of cell-mediated matrix remodeling on the cytotoxic effect of immobilized NYQQNC peptide to PANC-1 cells grown in hydrogels. After 10-day culture, PANC-1 cells formed clusters in soft PEG-MMP_{Linker} hydrogels independent of immobilized NYQQNC concentration (Figure 3A left panel, and B). When 4 mM NYQQNC was immobilized in stiff gels, however, very limited viable PANC-1 cells were observed (Figure 3A right panel, and C). This result was not surprising, since we have shown that NYQQNC peptide exhibited cytotoxic effect to PANC-1 cells encapsulated in stiff hydrogels 1-day postencapsulation (Figure 2). Interestingly, however, when a non-MMP sensitive linker (i.e., DTT) was used to cross-link hydrogels, PANC-1 cell viability and metabolic activity were unaffected regardless of gel stiffness or NYQQNC peptide concentration (Figure 3D−F and Figure S4, Supporting Information). Note that the metabolic activity of cells encapsulated in stiff PEG-MMP_{Linker} hydrogels still increased after 10-day culture (comparing Figures 2B and 3C) while it remained relatively constant in stiff PEG-DTT gels (Figure S4, Supporting Information).

Effect of Immobilized NYQQN Peptide Dosage on PANC-1 Cell Viability in Hydrogels. In order to evaluate the relation between NYQQNC peptide dosage and matrix stiffness on PANC-1 cell viability in 3D, we encapsulated PANC-1 cells at a higher cell density (5×10^6 cells/mL) since cells at a lower density (2×10^6 cells/mL) had very low viability in stiff hydrogels even without the presence of NYQQNC peptide (Figures 2B and 3C). Figure 4 shows the initial cell metabolic activity (2 h postencapsulation) in PEG-MMP_{Linker} hydrogels prepared without or with 4 mM NYQQNC. Clearly, the initial cell metabolic activity decreased with increasing stiffness and it was consistent with the live/dead staining images (Figure S5, Supporting Information). While initial cell viability decreased in stiffer gels (e.g., ∼93, ∼77, and ∼58% live cells in soft, medium, and stiff gels, respectively), more than half of the cells remained alive. Furthermore, significant decrease in initial metabolic activity was observed only in stiff gel immobilized with 4 mM

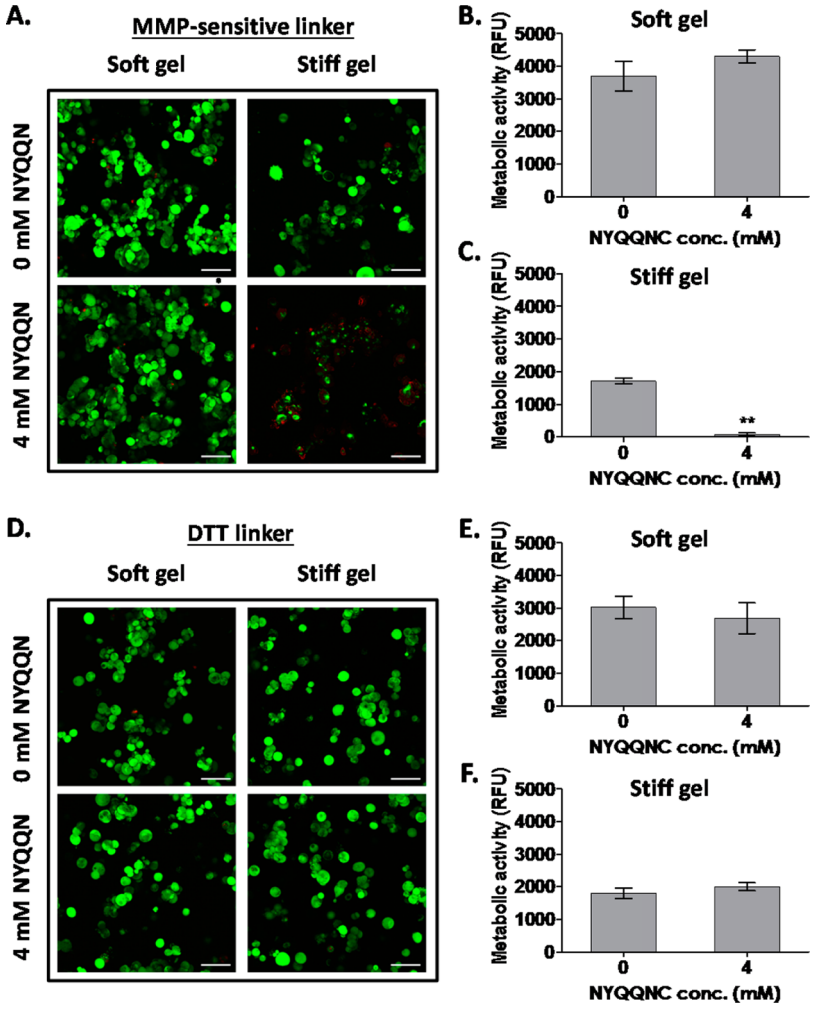

Figure 3. Representative live/dead staining images (A, D) and encapsulated PANC-1 cell (2×10^6 cells/mL) metabolic activity (B, C, E, F) in thiol−ene hydrogels with different conditions at day-10: (A−C) PEG-MMP_{Linker} gels; (D-F) PEG-DTT gels (scale: 100 μm, $n = 3$, $^{**}p < 0.01$).

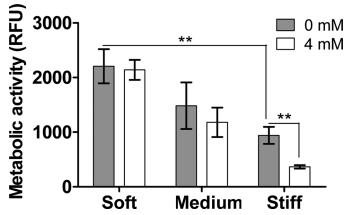

Figure 4. Initial metabolic activities of encapsulated PANC-1 cells (5×10^6 cells/ml) encapsulated in PEG-MMP_{Linker} hydrogels with different stiffness (see Table 1) and concentrations of immobilized NYQQNC (i.e., 0 or 4 mM). Metabolic activity was measured 2 h postencapsulation ($n = 3$, $^{**}p < 0.01$).

NYQQNC peptide. The remaining viable cells continued to grow and caused significant reduction in thiol−ene hydrogel stiffness after 10-day culture (Table 1). Gels prepared with higher PEG8NB concentration exhibited higher initial moduli and cross-linking density, but the presence of cells reduced gel moduli. Table 2 shows similar studies using noncleavable DTT as the gel cross-linker. The stiffness of all hydrogels decreased after 10-day culture, especially in MMP-sensitive hydrogels encapsulated with cells. The percentage reductions of gel shear moduli were higher in cell-laden and MMP-sensitive gels (43−58%) than in DTT-cross-linked hydrogels (13−20%). Note that soft gels degraded faster than stiff gels due to accelerated hydrolytic gel degradation in gels with lower PEG8NB content. This result is similar to our previous observation.[53]

As shown in Figure 5A, immobilized NYQQNC peptide affected cell metabolic activity in the soft hydrogels very minimally only when 4 mM of NYQQNC was immobilized (statistical significance was only obtained at day 4 and day 10). In hydrogels with medium stiffness, cell metabolic activity was affected to a higher degree at 4 mM immobilized NYQQN peptide (Figure 5B). The metabolic activity of cells encapsulated in stiff hydrogels was significantly suppressed in the presence of 2 or 4 mM immobilized NYQQNC peptide (Figure 5C). Comparing Figure 4 (2 h postencapsulation) and Figure 5B (1 day postencapsulation), it was clear that immobilized NYQQNC peptide exhibited increasing cytotoxicity to the encapsulated cells in the medium stiffness gels. In these gels, no cytotoxic effect was observed 2 h postencapsulation but significant reduction in metabolic activity could be seen 1 day postencapsulation. Figure 6 shows the morphology of encapsulated cells 10 days postencapsulation using the same gel formulations shown in Figure 5. While cells proliferated to form clusters in soft hydrogels at all NYQQNC concentrations, limited viable cells were observed in 4 mM NYQQN-immobilized hydrogels with medium stiffness and almost no viable cell was observed in 2 or 4 mM peptide immobilized stiff hydrogels. When the cells were coencapsulated with soluble

dx.doi.org/10.1021/bm4004496 | Biomacromolecules 2013, 14, 3017−3026

Table 1. Effect of Encapsulated PANC-1 Cells (5×10^6 cells/mL) on Shear Moduli and Cross-Linking Densities of PEG-MMP_{Linker} Hydrogels (n = 3, mean ± SD)

		no cells			with cells		
PEG8NB (wt %)		4 (soft)	6 (medium)	8 (stiff)	4 (soft)	6 (medium)	8 (stiff)
G' (kPa)	D0	2.0 ± 0.1	8.5 ± 1.0	18.4 ± 0.5	1.9 ± 0.1	6.7 ± 0.4	11.8 ± 1.0
	D10	1.4 ± 0.2	6.8 ± 0.6	13.6 ± 0.2	0.8 ± 0.1	3.6 ± 0.3	6.7 ± 0.3
ρ (mM)	D0	0.78 ± 0.04	3.30 ± 0.39	7.14 ± 0.19	0.74 ± 0.04	2.60 ± 0.16	4.58 ± 0.39
	D10	0.54 ± 0.06	2.63 ± 0.22	5.26 ± 0.07	0.31 ± 0.04	1.40 ± 0.12	2.60 ± 0.12
	reduction	31%	20%	26%	58%	46%	43%

Table 2. Effect of Encapsulated PANC-1 cells (5×10^6 cells/mL) on Shear Moduli and Cross-Linking Densities of PEG-DTT Hydrogels (n = 3, mean ± SD)

		no cells			with cells		
PEG8NB (wt %)		4 (soft)	6 (medium)	8 (stiff)	4 (soft)	6 (medium)	8 (stiff)
G' (kPa)	D0	1.1 ± 0.1	7.0 ± 0.2	14.3 ± 0.7	1.0 ± 0.2	6.0 ± 0.4	13.3 ± 0.5
	D10	0.5 ± 0.1	4.8 ± 0.4	10.8 ± 0.6	0.8 ± 0.1	5.0 ± 0.2	11.6 ± 0.4
ρ (mM)	D0	0.43 ± 0.04	2.72 ± 0.08	5.55 ± 0.27	0.39 ± 0.08	2.33 ± 0.16	5.16 ± 0.19
	D10	0.19 ± 0.04	1.86 ± 0.16	4.19 ± 0.23	0.31 ± 0.04	1.94 ± 0.08	4.50 ± 0.16
	reduction	55%	31%	24%	20%	17%	13%

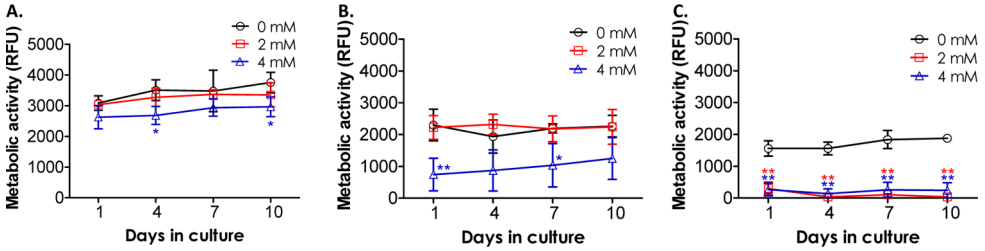

Figure 5. Effect of matrix stiffness and NYQQNC peptide on metabolic activity of PANC-1 cells encapsulated (5×10^6 cells/mL) in PEG-MMP_{Linker} gels with different stiffness: (A) soft, (B) medium, and (C) stiff (n = 3, *p < 0.05, **p < 0.01, compared to 0 mM peptide in each stiffness group at the same time point).

NYQQN peptide (without cysteine residue) and cultured media supplemented with 4 mM soluble NYQQN peptide, similar reduction in cellular metabolic activity was observed only in stiff gel. The presence of integrin ligand CRGDS (1 mM) in hydrogel did not rescue cells from cytotoxic effect of NYQQN peptide (Figure S6, Supporting Information).

Effect of Immobilized NYQQN Peptide on PANC-1 Cell Apoptosis. To understand the mechanism by which immobilized NYQQNC peptide affects cell viability, we examined activation of caspases in the encapsulated PANC-1 cells two hours postencapsulation (Figure 7). We chose gels with medium stiffness ($G' \sim 6.7$ kPa) for immunostaining of caspases because this formulation contained more viable cells for easy visualization of cells containing activated caspases and the fact that the PANC-1 cells encapsulated in this gel formulation were still susceptible to NYQQNC-mediated toxicity. Representative caspases immunofluorescence staining images show strong staining of caspases only in cells encapsulated in hydrogels immobilized with 4 mM of NYQQNC peptide (Figure 7A). We also evaluated activated caspase activities in cell-laden soft, medium, or stiff hydrogels using a more quantitative CaspasGlo 3/7 reagent (Figure 7B-7D). Results show that the degree of caspase 3/7 activation reached statistical significance only in the stiff hydrogels (Figure 7D).

Expression Levels of EGFR and Akt. Although NYQQN peptide was proposed as an EGFR inhibitor, its effects on pancreatic tumor cells have not been studied. Using Western blotting, we examined the effect of NYQQN peptide on related protein expression (EGFR and Akt) in PANC-1 cells cultured on TCP (2D) or in PEG-peptide hydrogels (3D). In 2D culture (Figure 8A–C), soluble NYQQN peptide treatment did not cause significant changes in relative expression levels of EGFR but slightly reduced (not statistically significant) Akt expression after 3 days. This result agrees with our 2D cell viability assays as shown in Figure S3 in the Supporting Information. In 3D culture without NYQQNC peptide (Figure 8D–F), EGFR and Akt protein expression levels were decreased slightly in stiff hydrogels one-day postencapsulation. The immobilization of NYQQNC peptide at 4 mM in stiff hydrogels significantly decreased relative EGFR and Akt expression in the encapsulated cells and the suppression effect persisted throughout the 10-day study (Figure 8G–I).

DISCUSSION

The influence of EGFR inhibition on tumor cell growth has been studied extensively due to the importance of EGFR

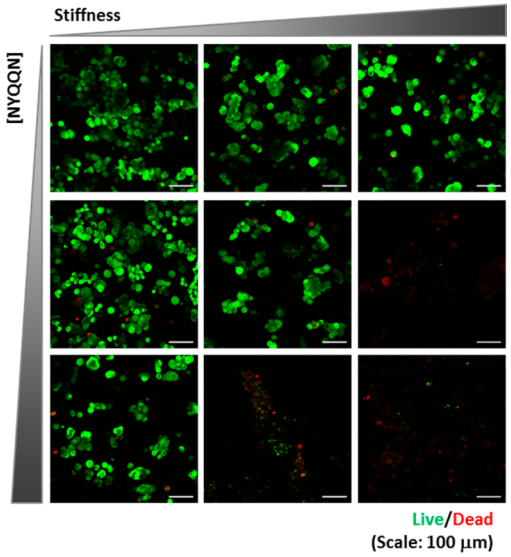

Figure 6. Representative day-10 live/dead staining images of PANC-1 cells (5×10^6 cells/mL) encapsulated in PEG-MMP_{Linker} hydrogels with varying stiffness (from left to right: soft, medium, and stiff gels) and immobilized NYQQNC peptide concentration (from top to bottom: 0, 2, and 4 mM).

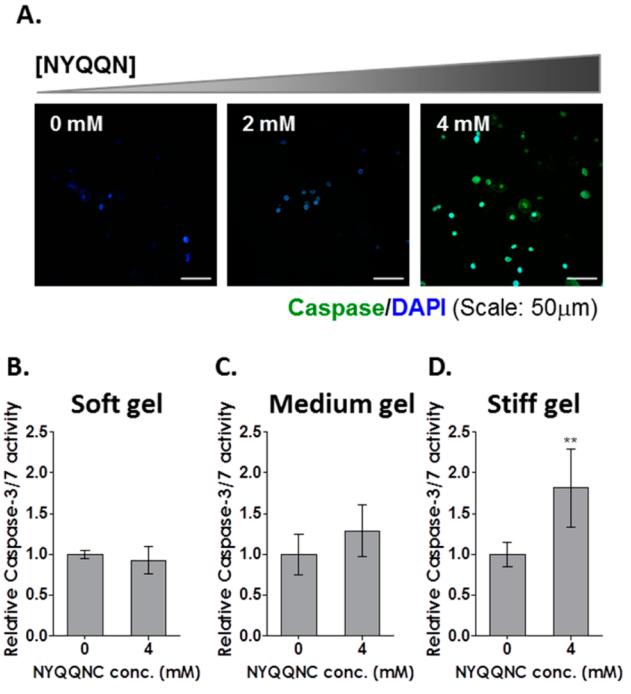

Figure 7. (A) Representative CaspaACE in situ marker staining images performed at day 0. PANC-1 cells were encapsulated (5×10^6 cells/mL) in 6 wt % PEG-MMP_{Linker} hydrogels immobilized with different concentrations of NYQQNC (activated capases, green; DAPI, blue). (B–D) Relative caspase-3/7 activities in PANC-1 cells encapsulated in PEG-MMP_{Linker} hydrogels with 0 or 4 mM NYQQNC peptide at day 0 ($n = 3$, $^{**}p < 0.01$).

signaling in cell proliferation and metastasis. However, most of these studies were conducted on conventional 2D cell culture substrates. Cells adhered to the top of the substrate surface are unnaturally polarized and do not receive signals delivered from the tumor microenvironment. Therefore, appropriate 3D culture platforms capable of decoupling various matrix properties should help in assessing cancer cell fate in a more relevant microenvironment. In this study, we designed tunable PEG-peptide hydrogels as a 3D platform to study the effect of EGFR peptide antagonist (NYQQN) on PANC-1 cell survival and proliferation. The thiol–ene PEG-peptide hydrogels used here had a wide range of stiffness (~1–18 kPa) and protease sensitivity. The range of stiffness used here was pathophysiologically relevant since the moduli of soft hydrogels match that of normal pancreatic tissue[50,51] and the moduli of medium and stiff gels are relevant to that of tumor tissues.[52] Without the presence of cells, all gels degraded slowly due to gel swelling and hydrolysis of ester bonds between PEG backbone and norbornene groups.[53] The presence of cells during network cross-linking reduced initial gel moduli because of the disruption of local polymer cross-linking and the creation of voids due to the presence of cells.[54] This phenomenon was more noticeable in MMP-sensitive hydrogels, potentially due to the cleavage of peptide linker during gel cross-linking and prior to rheometrical measurement (~2 h). The initial cell viability was found to be lower in stiffer hydrogels, likely due to a highly cross-linked network structure that imposed higher environmental stresses to the cells. These cells, however, proliferated to form small clusters and caused higher degree of gel degradation, especially in MMP-sensitive hydrogels (Tables 1 and 2). Note that these cells were encapsulated initially as single cells and the hydrogel matrix contained no cell adhesive motifs (e.g., RGD). Future work will explore the influence of immobilized cell adhesive motifs on the survival, migration, and proliferation of cells encapsulated either as single cells or as tumor spheres.

A potential antitumor peptide drug, NYQQN, inhibits autophosphorylation of EGFR-TK by hindering ATP access to a catalyst loop in TK.[10] Studies have shown that it inhibits EGFR-mediated signaling in an ATP-independent manner. Interestingly, our results showed that soluble NYQQN peptide has no growth inhibition or cytotoxic effect on PANC-1 cells cultured on TCP with concentrations up to 8 mM (Figure S3, Supporting Information). When immobilized in hydrogels, NYQQN peptide did not cause cell death in hydrogels with lower stiffness (Figure 2A) or cross-linked by noncleavable DTT (Figure S4, Supporting Information and Figure 3). PANC-1 cell viability in 3D culture, however, was greatly suppressed by soluble or immobilized NYQQN peptide (at 4 mM) in hydrogels with higher stiffness *and* MMP sensitivity (Figures 2B, 3, and S6B). Interestingly, the addition of integrin ligand CRGDS did not rescue cells from cytotoxic effect induced by higher matrix stiffness or NYQQN peptide (Figure S6B, Supporting Information). While it is possible that additional thiol–ene reaction contributed to NYQQN peptide cytotoxicity, this was not the case in DTT-cross-linked gels. The fact that NYQQN peptide did not affect cell survival in both soft and stiff PEG hydrogels cross-linked by DTT implies that the cytotoxic effect of this peptide was not due to additional thiol–ene reaction during encapsulation. Rather, the cytotoxic effect was relevant to local matrix conditions, including gel stiffness and protease sensitivity. This could also explain why the peptide failed to induce cell death when cultured on TCP. The mechanisms leading to this interesting result may be relevant to differences in cell morphology or intracellular signaling elicited by gels with different compositions. Further studies are required to elucidate the exact mechanisms.

Cell–cell interaction is critical in maintaining viability and functions of certain cells in PEG-based hydrogels.[55] PANC-1

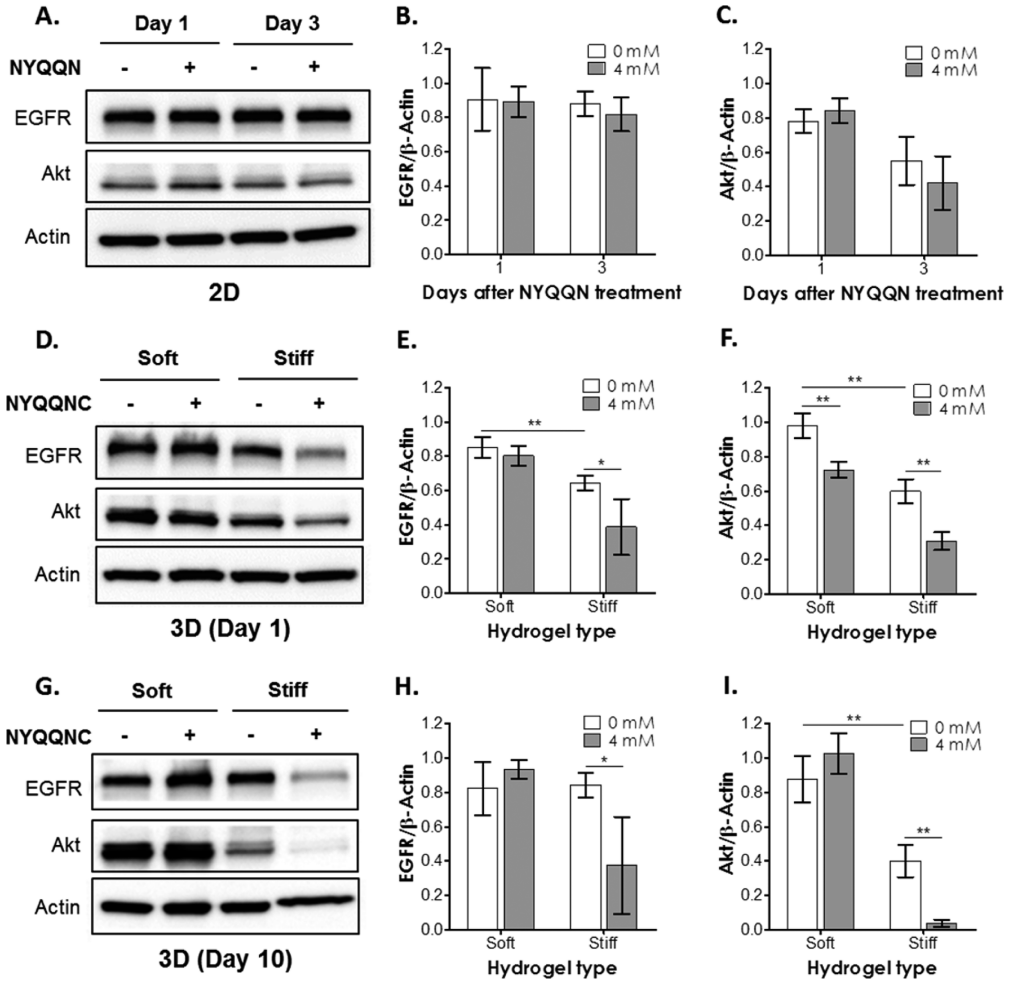

Figure 8. Western blotting (A, D, G) and band intensity analysis (B, C, E, F, H, I) for EGFR and Akt expressions in 2D culture (A–C) or 3D culture for 1 day (D–F) and 10 days (G–I) (n = 3, *p < 0.05, **p < 0.01).

cells exhibited higher initial viability when encapsulated in thiol–ene PEG-peptide hydrogels at a higher density (e.g., 5 × 10^6 cells/mL). This allowed us to evaluate the dosing effect of immobilized NYQQNC peptide on the encapsulated cells, especially in stiffer hydrogels. While cell viability was minimally affected by the immobilized NYQQNC peptide in softer gels, lower concentrations of NYQQNC were sufficient to induce cell death in gels with higher stiffness (Figures 5 and 6). It is possible that EGFR inhibition down-regulates cell survival pathway PI3K-Akt and causes apoptosis.[13,26,56] We found that cell death induced by this peptide in stiffer hydrogels was a result of cell apoptosis (Figure 7) and the mechanism may be related to the expression levels of EGFR and Akt (Figure 8). While soluble NYQQN peptide treatment in 2D culture did not significantly alter the expression of these two proteins, differences were observed in 3D matrices with different stiffness. Without immobilized NYQQN peptide, the expression of EGFR in PANC-1 cells encapsulated in 3D hydrogels was slightly decreased in stiff hydrogels initially (Figure 8E). The difference in EGFR expression, however, diminished after 10 days of 3D culture (Figure 8H). It was likely that increased cell–cell interactions as time restored EGFR expression. Further, we found that the expression of EGFR was largely affected by the immobilization of NYQQNC in stiff hydrogels (Figure 8D, E, G, H). PANC-1 cell-secreted or trace amount of EGF in the FBS supplemented in the culture media could alter the sensitivity and susceptibility of EGFR in the stiff hydrogels. In contrast to EGFR, the expression of Akt in PANC-1 cells appeared to be more sensitive to 3D matrix conditions, especially in stiffer matrices (Figure 8D, F, G, I). This could explain lower cell viability found in stiffer hydrogels. Since Akt is an intracellular protein kinase whose expression is affected by many growth factors, it is likely that other Akt-related signaling pathways are differentially activated or inhibited in PDAC cells cultured in 3D matrix with different biophysical and biochemical properties.

Although we have evaluated the stiffness-dependent cytotoxic effect of NYQQN peptide on pancreatic cancer cells, it is not clear why this peptide only suppressed the expression of EGFR and Akt in PANC-1 cells encapsulated in stiff hydrogels, and future studies are required to discover the underlying mechanisms. Nonetheless, the highly adaptable material platform utilized in this contribution offers many unique advantages over conventional 2D cell culture or animal-derived 3D matrices. In addition to matrix stiffness, protease sensitivity, and receptor inhibition effects studied here, future work will also focus on the influence of exogenously added growth factors (e.g., EGF, TGF-β1, etc.) and cell-adhesive motifs (e.g., collagen or laminin-derived integrin-binding peptides) on the growth and migration of tumor cells in 3D.

dx.doi.org/10.1021/bm4004496 | Biomacromolecules 2013, 14, 3017–3026

CONCLUSIONS

In conclusion, we have shown that PEG-peptide hydrogels formed by thiol−ene photoclick reaction serve as a promising platform for 3D culture of pancreatic cancer cells. We show that the viability of PDAC cells under the influence of EGFR inhibition was altered not only by the dose of the inhibitor, but also by the conditions of the matrix in which the cells reside. Our studies also show that an ineffective drug in 2D PDAC cell culture (e.g., NYQQN peptide) may exhibit cytotoxic effect in biomimetic 3D matrices. Furthermore, the use of 3D hydrogel matrices with adaptable and well-defined biophysical and biochemical properties may facilitate the identification of anticancer drugs that are effective in tumor tissues but with minimal side effects to normal tissues.

ASSOCIATED CONTENT

Supporting Information

Effect of pendent peptide on hydrogel stiffness, total DNA content, and dosage effects of NYQQN on PANC-1 cell cultured in 2D and 3D. This material is available free of charge via the Internet at http://pubs.acs.org.

AUTHOR INFORMATION

Corresponding Author

*E-mail: lincc@iupui.edu.

Notes

The authors declare no competing financial interest.

ACKNOWLEDGMENTS

This project was supported by a faculty start-up fund from IUPUI Department of Biomedical Engineering and a pilot grant from IUPUI Biomechanics & Biomaterials Research Center (BBRC). The authors thank Asad Raza and Dr. Hiroki Yokota for their technical assistance and Dr. Murray Korc for helpful discussion related to pancreatic cancer cells.

REFERENCES

(1) Lee, J.; Jang, K. T.; Ki, C. S.; Lim, T.; Park, Y. S.; Lim, H. Y.; Choi, D. W.; Kaing, W. K.; Park, K.; Park, J. O. *Cancer* **2007**, *109*, 1561−1569.
(2) Michl, P.; Gress, T. M. *Gut* **2013**, *62*, 317−326.
(3) Wachsmann, M. B.; Pop, L. M.; Vitetta, E. S. *J. Invest. Med.* **2012**, *60*, 643−663.
(4) Chang, Z. G.; Wei, J. M.; Qin, C. F.; Hao, K.; Tian, X. D.; Xie, K.; Xie, X. H.; Yang, Y. M. *Dig. Dis. Sci.* **2012**, *57*, 1181−1189.
(5) Deharvengt, S.; Marmarelis, M.; Korc, M. *PloS One* **2012**, *7*, e39684.
(6) Kelley, R. K.; Ko, A. H. *Biol.: Targets Ther.* **2008**, *2*, 83−95.
(7) Azzariti, A.; Porcelli, L.; Gatti, G.; Nicolin, A.; Paradiso, A. *Biochem. Pharmacol.* **2008**, *75*, 1035−1044.
(8) Claperon, A.; Guedj, N.; Mergey, M.; Vignjevic, D.; Desbois-Mouthon, C.; Boissan, M.; Saubamea, B.; Paradis, V.; Housset, C.; Fouassier, L. *Oncogene* **2012**, *31*, 1376−1388.
(9) Paez, J. G.; Janne, P. A.; Lee, J. C.; Tracy, S.; Greulich, H.; Gabriel, S.; Herman, P.; Kaye, F. J.; Lindeman, N.; Boggon, T. J.; Naoki, K.; Sasaki, H.; Fujii, Y.; Eck, M. J.; Sellers, W. R.; Johnson, B. E.; Meyerson, M. *Science* **2004**, *304*, 1497−1500.
(10) Abe, M.; Kuroda, Y.; Hirose, M.; Kato, M.; Murakami, M.; Watanabe, Y.; Nakano, M.; Handa, T. *Biopolymers* **2008**, *89*, 40−51.
(11) Cardo-Vila, M.; Giordano, R. J.; Sidman, R. L.; Bronk, L. F.; Fan, Z.; Mendelsohn, J.; Arap, W.; Pasqualini, R. *Proc. Natl. Acad. Sci. U.S.A.* **2010**, *107*, 5118−5123.
(12) Ciardiello, F.; Tortora, G. *New Engl. J. Med.* **2008**, *358*, 1160−1174.
(13) Henson, E. S.; Gibson, S. B. *Cell. Signalling* **2006**, *18*, 2089−2097.
(14) Derer, S.; Bauer, P.; Lohse, S.; Scheel, A. H.; Berger, S.; Kellner, C.; Peipp, M.; Valerius, T. *J. Immunol.* **2012**, *189*, 5230−5239.
(15) Meng, E. C.; Shoichet, B. K.; Kuntz, I. D. *J. Comput. Chem.* **1992**, *13*, 505−524.
(16) Mills, J. E. J.; Dean, P. M. *J. Comput.-Aided Mol. Des.* **1996**, *10*, 607−622.
(17) Niv, M. Y.; Rubin, H.; Cohen, J.; Tsirulnikov, L.; Licht, T.; Peretzman-Shemer, A.; Cna'an, E.; Tartakovsky, A.; Stein, I.; Albeck, S.; Weinstein, I.; Goldenberg-Furmanov, M.; Tobi, D.; Cohen, E.; Laster, M.; Ben-Sasson, S. A.; Reuveni, H. *J. Biol. Chem.* **2004**, *279*, 1242−1255.
(18) D'Andrea, L. D.; Del Gatto, A.; Pedone, C.; Benedetti, E. *Chem. Biol. Drug Des.* **2006**, *67*, 115−126.
(19) Hidalgo, M.; Eckhardt, S. G. *J. Natl. Cancer Inst.* **2001**, *93*, 178−193.
(20) Vagner, J.; Qu, H.; Hruby, V. J. *Curr. Opin. Chem. Biol.* **2008**, *12*, 292−296.
(21) Cukierman, E.; Pankov, R.; Stevens, D. R.; Yamada, K. M. *Science* **2001**, *294*, 1708−1712.
(22) Debnath, J.; Brugge, J. S. *Nat. Rev. Cancer* **2005**, *5*, 675−688.
(23) Miroshnikova, Y. A.; Jorgens, D. M.; Spirio, L.; Auer, M.; Sarang-Sieminski, A. L.; Weaver, V. M. *Phys. Biol.* **2011**, *8*, 026013.
(24) Pek, Y. S.; Wan, A. C. A.; Ying, J. Y. *Biomaterials* **2010**, *31*, 385−391.
(25) Peyton, S. R.; Raub, C. B.; Keschrumrus, V. P.; Putnam, A. J. *Biomaterials* **2006**, *27*, 4881−4893.
(26) Leight, J. L.; Wozniak, M. A.; Chen, S.; Lynch, M. L.; Chen, C. S. *Mol. Biol. Cell* **2012**, *23*, 781−791.
(27) Levental, K. R.; Yu, H.; Kass, L.; Lakins, J. N.; Egeblad, M.; Erler, J. T.; Fong, S. F. T.; Csiszar, K.; Giaccia, A.; Weninger, W.; Yamauchi, M.; Gasser, D. L.; Weaver, V. M. *Cell* **2009**, *139*, 891−906.
(28) Kim, J. H.; Asthagiri, A. R. *J. Cell Sci.* **2011**, *124*, 1280−1287.
(29) Chitcholtan, K.; Asselin, E.; Parent, S.; Sykes, P. H.; Evans, J. J. *Exp. Cell Res.* **2013**, *319*, 75−87.
(30) Sempere, L. F.; Gunn, J. R.; Korc, M. *Cancer Biol. Ther.* **2011**, *12*, 198−207.
(31) Chen, G. P.; Ushida, T.; Tateishi, T. *Macromol. Biosci.* **2002**, *2*, 67−77.
(32) Drury, J. L.; Mooney, D. J. *Biomaterials* **2003**, *24*, 4337−4351.
(33) Hutmacher, D. W. *Biomaterials* **2000**, *21*, 2529−2543.
(34) Park, S. Y.; Ki, C. S.; Park, Y. H.; Jung, H. M.; Woo, K. M.; Kim, H. J. *Tissue Eng., Part A* **2010**, *16*, 1271−1279.
(35) Tibbitt, M. W.; Anseth, K. S. *Biotechnol. Bioeng.* **2009**, *103*, 655−663.
(36) Burdick, J. A.; Anseth, K. S. *Biomaterials* **2002**, *23*, 4315−4323.
(37) Hern, D. L.; Hubbell, J. A. *J. Biomed. Mater. Res.* **1998**, *39*, 266−276.
(38) Lutolf, M. P.; Lauer-Fields, J. L.; Schmoekel, H. G.; Metters, A. T.; Weber, F. E.; Fields, G. B.; Hubbell, J. A. *Proc. Natl. Acad. Sci. U.S.A.* **2003**, *100*, 5413−5418.
(39) Chung, I. M.; Enemchukwu, N. O.; Khaja, S. D.; Murthy, N.; Mantalaris, A.; Garcia, A. J. *Biomaterials* **2008**, *29*, 2637−2645.
(40) Kraehenbuehl, T. P.; Zammaretti, P.; Van der Vlies, A. J.; Schoenmakers, R. G.; Lutolf, M. P.; Jaconi, M. E.; Hubbell, J. A. *Biomaterials* **2008**, *29*, 2757−2766.
(41) Sieh, S.; Taubenberger, A. V.; Rizzi, S. C.; Sadowski, M.; Lehman, M. L.; Rockstroh, A.; An, J.; Clements, J. A.; Nelson, C. C.; Hutmacher, D. W. *PloS One* **2012**, *7*, e40217.
(42) Weiss, M. S.; Bernabe, B. P.; Shikanov, A.; Bluver, D. A.; Mui, M. D.; Shin, S.; Broadbelt, L. J.; Shea, L. D. *Biomaterials* **2012**, *33*, 3548−3559.
(43) Yang, X.; Sarvestani, S. K.; Moeinzadeh, S.; He, X.; Jabbari, E. *Tissue Eng., Part A* **2013**, *19*, 669−684.
(44) Aimetti, A. A.; Machen, A. J.; Anseth, K. S. *Biomaterials* **2009**, *30*, 6048−6054.
(45) Lin, C. C.; Raza, A.; Han, S. *Biomaterials* **2011**, *32*, 9685−9695.

(46) Fairbanks, B. D.; Schwartz, M. P.; Halevi, A. E.; Nuttelman, C. R.; Bowman, C. N.; Anseth, K. S. *Adv. Mater.* **2009**, *21*, 5005−5010.
(47) Benton, J. A.; Fairbanks, B. D.; Anseth, K. S. *Biomaterials* **2009**, *30*, 6593−6603.
(48) Patterson, J.; Hubbell, J. A. *Biomaterials* **2010**, *31*, 7836−7845.
(49) Rubinstein, M. In *Polymer Physics*; Rubinstein, M., Colby, R. H., Eds.; Oxford University Press: New York, 2003; p 259.
(50) Arda, K.; Ciledag, N.; Aktas, E.; Aribas, B. K.; Köse, K. *Am. J. Roentgenol.* **2011**, *197*, 532−536.
(51) Botta, G. P.; Reichert, M.; Reginato, M. J.; Heeg, S.; Rustgi, A. K.; Lelkes, P. I. *Neoplasia* **2013**, *15*, 359−372.
(52) Krouskop, T. A.; Wheeler, T. M.; Kallel, F.; Garra, B. S.; Hall, T. *Ultrason. Imaging* **1998**, *20*, 260−274.
(53) Shih, H.; Lin, C. C. *Biomacromolecules* **2012**, *13*, 2003−2012.
(54) Lee, W.; Cho, N. J.; Xiong, A.; Glenn, J. S.; Frank, C. W. *Proc. Natl. Acad. Sci. U.S.A.* **2010**, *30*, 20709−20714.
(55) Lin, C. C.; Anseth, K. S. *Proc. Natl. Acad. Sci. U.S.A.* **2011**, *108*, 6380−6385.
(56) Franke, T. F.; Kaplan, D. R.; Cantley, L. C. *Cell* **1997**, *88*, 435−437.

Effect of 3D matrix compositions on the efficacy of EGFR inhibition in pancreatic ductal adenocarcinoma cells

Chang Seok Ki, Han Shih, and Chien-Chi Lin*
Department of Biomedical Engineering, Purdue School of Engineering and Technology,
Indiana-University Purdue-University at Indianapolis, IN 46202, USA

(Supporting Figures)

*To whom correspondence should be addressed:

Chien-Chi Lin, PhD.
Assistant Professor
Department of Biomedical Engineering
Purdue School of Engineering and Technology
Indiana University-Purdue University at Indianapolis
Indianapolis, IN 46202
Email: lincc@iupui.edu

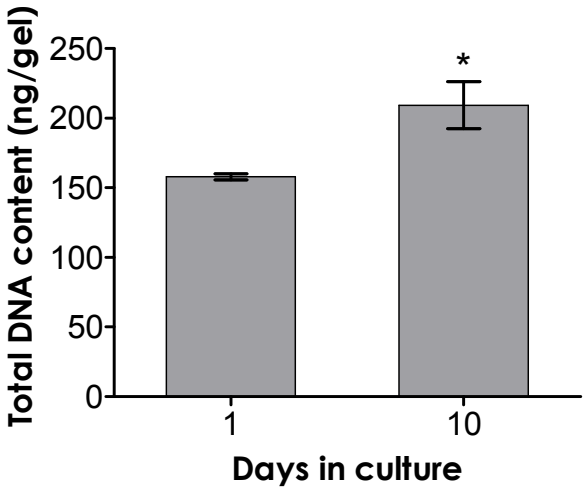

Figure S1. Total DNA content of PANC-1 cells encapsulated in 4 wt.% PEG-MMP_{Linker} hydrogels for 1 day and 10 days. The initial cell density was 2×10^6 cells/mL (n = 3, * $p < 0.05$).

A.

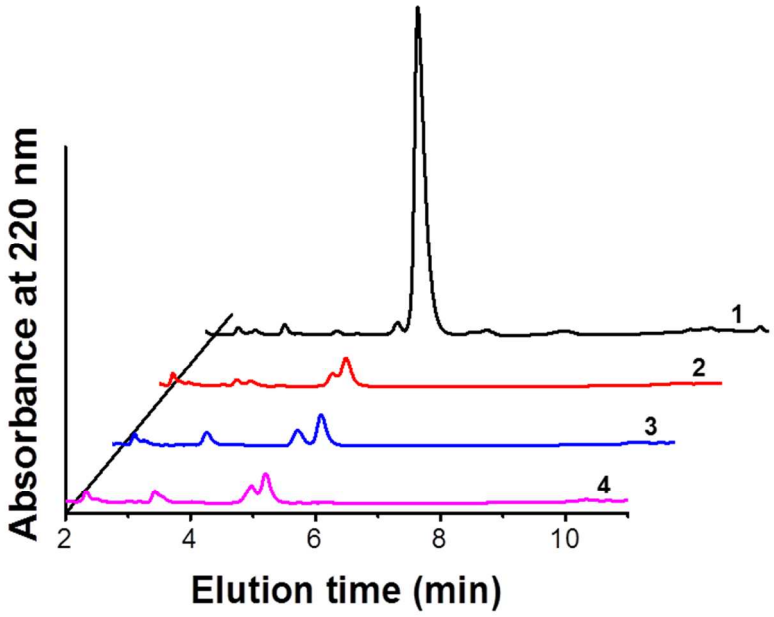

B.

[PEG8NB] (wt.%)	4	6	8
NYQQNC immobilization efficiency (%)	92 ± 3%	88 ± 4%	93 ± 1%

Figure S2. (A) Representative HPLC traces of NYQQNC peptide. Trace 1: 0.25 mM of soluble NYQQNC, a concentration equivalent to 0% immobilization (i.e., all 4 mM of NYQQNC peptide in a 25 μL gel release into 400 μL solution). Traces 2-3: solution samples containing NYQQNC peptides released from 4, 6, and 8 wt% PEG-DTT hydrogels after 24-hr incubation. The concentration of NYQQNC peptide in the pre-polymer solution was 4mM. (B) Peptide immobilization efficiency determined by normalizing areas under traces 2-4 to that of trace 1 (n = 3, mean ± SD).

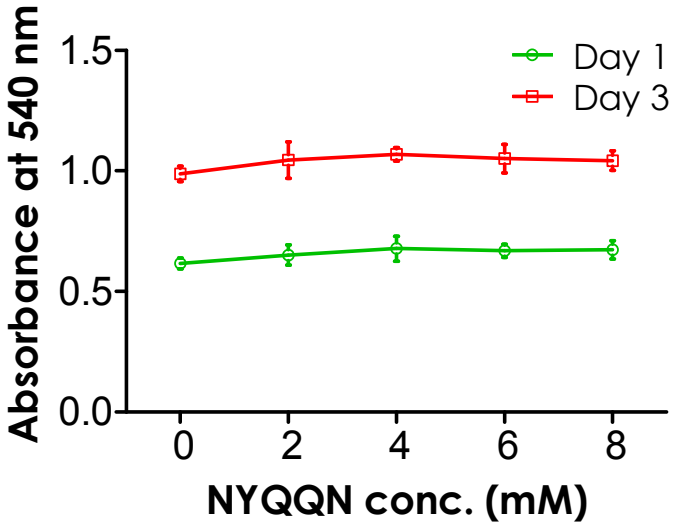

Figure S3. Effect of soluble EGFR inhibitor (NYQQN) on PANC-1 cell viability cultured in 2D. Cell viability was measured by MTT assay 1- and 3-days after drug treatment (n = 6, mean ± SD).

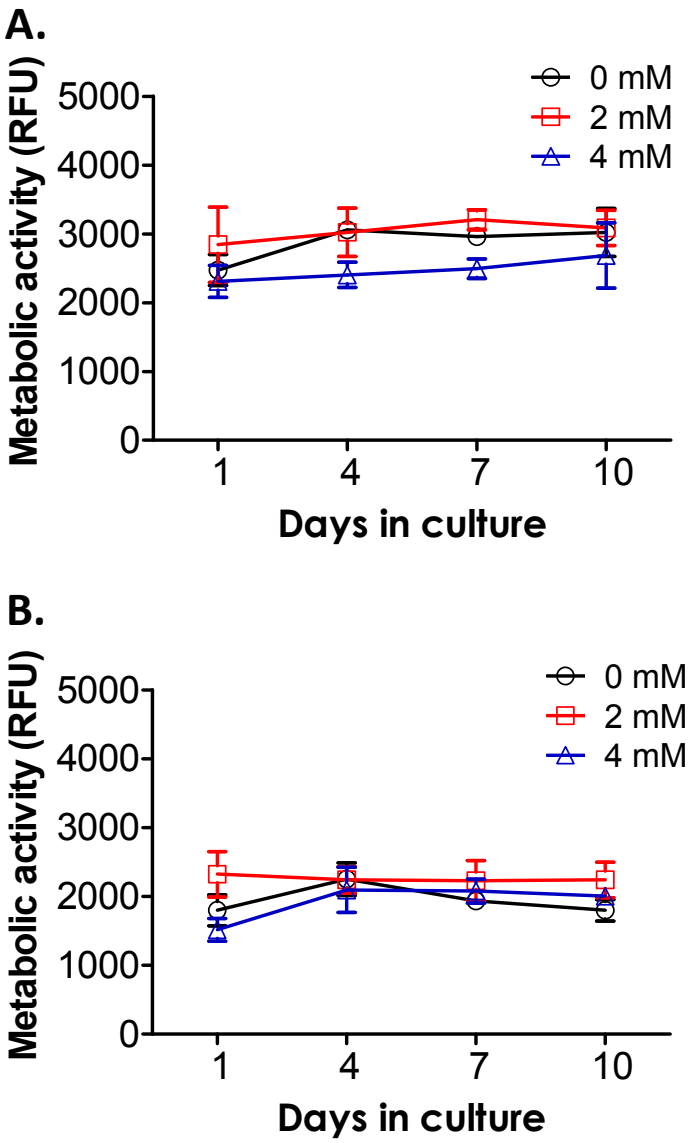

Figure S4. Effect of matrix stiffness and NYQQNC peptide on metabolic activity of PANC-1 cells encapsulated in soft (A) and stiff (B) PEG-DTT hydrogels. Stiffness (G'_0) in soft and stiff gels was 1.0 and 13.3 kPa, respectively. Cell metabolic activity was determined by AlamarBlue reagent. Initial cell density was 2×10^6 cells/mL (n = 3, mean ± SD).

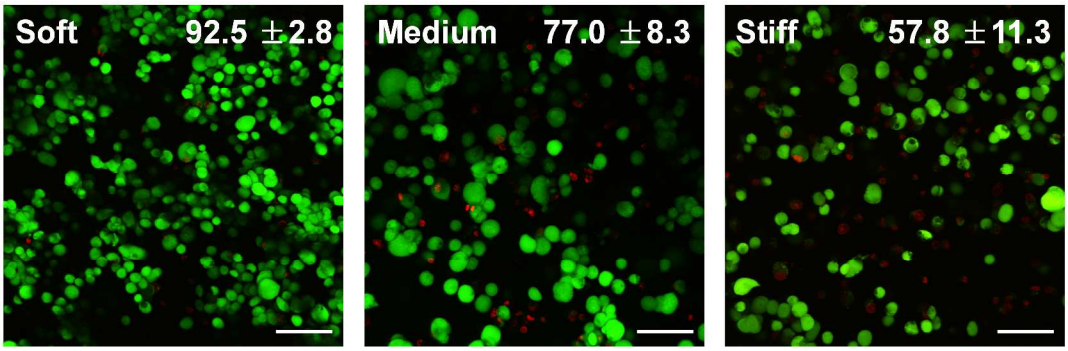

Figure S5. Representative live/dead staining images of PANC-1 cells (5×10^6 cells/mL) encapsulated in PEG-MMP_{Linker} hydrogels with different stiffness (see Table 1). Staining was performed 2 hours post-encapsulation (% live cells were labeled at the upper right corners in each image. Scale: 100 μm).

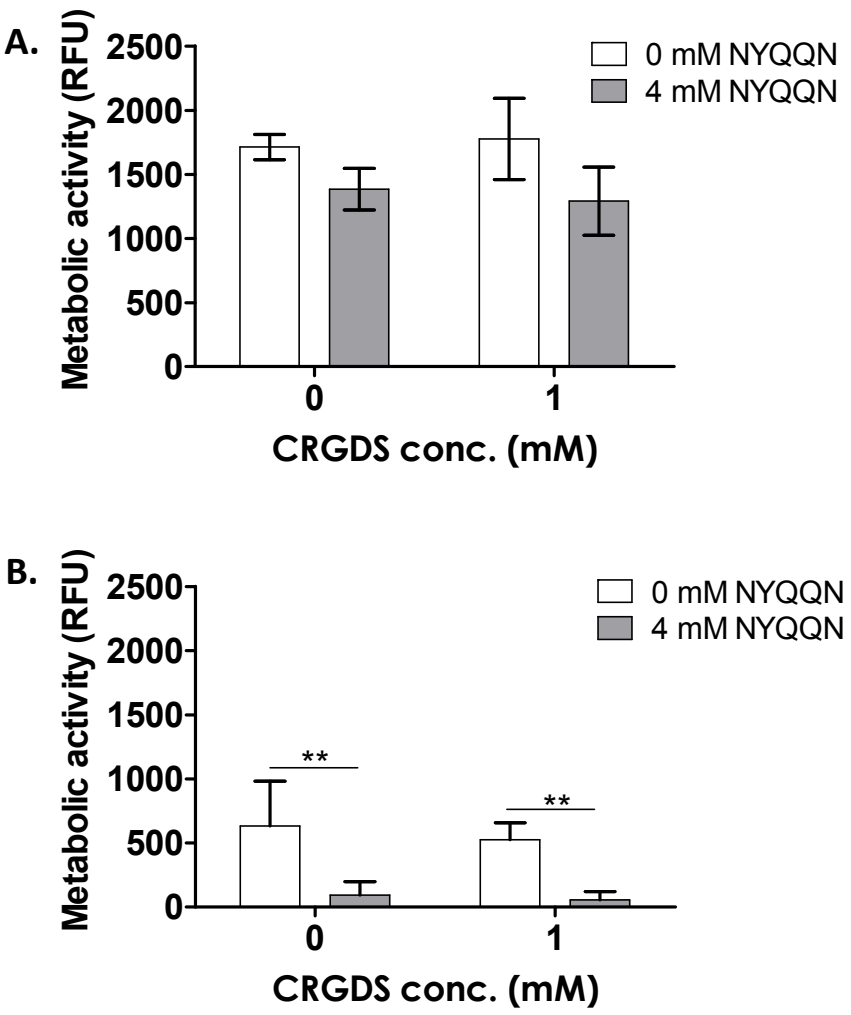

Figure S6. Effect of gel stiffness on metabolic activity of PANC-1 cell encapsulated in 0 or 1 mM CRGDS immobilized soft (A) and stiff (B) PEG-MMP_{Linker} hydrogels. Stiffness (G'_0) in soft and stiff gels was 1.0 and 13.3 kPa, respectively. Zero or four mM soluble NYQQN was added to pre-polymer solution during cell encapsulation and cell-laden gels were incubated in culture media supplemented with 4 mM soluble NYQQN. Metabolic activity was determined by AlamarBlue assay at day 1. Initial cell density was 5×10^6 cell/mL (n = 3, ** $P < 0.01$).

Table S1. Formulations of thiol-ene hydrogels used in this study. In each wt.% PEG8NB gel, the linker concentration (i.e., $[SH]_{from\ linker}$) was fixed regardless of NYQQNC peptide concentration (0, 2, or 4 mM).

PEG8NB (wt.%)	**4 (soft)**	**6 (medium)**	**8 (stiff)**
[PEG8NB] (mM)	2	3	4
[ene] (mM)	16	24	32
[Linker] (mM)	6	10	14
$[SH]_{from\ linker}$ (mM)	12	20	28

Table S2. Shear moduli and cross-linking densities of PEG-peptide hydrogels prepared in the absence or presence of NYQQNC pendent peptide (0 or 4 mM). ** $p < 0.01$ (compared to 0 mM NYQQNC at the same time point, n = 3, mean ± SD).

PEG8NB (wt.%)		**4 (soft)**		**6 (medium)**		**8 (stiff)**	
NYQQNC (mM)		**0**	**4**	**0**	**4**	**0**	**4**
G' (kPa)	**D0**	2.0 ± 0.1	2.1 ± 0.1	8.5 ± 1.0	7.9 ± 1.2	18.4 ± 0.5	16.6 ± 1.8
	D1	1.8 ± 0.1	1.8 ± 0.5	7.5 ± 0.6	7.4 ± 0.6	14.2 ± 0.2	17.3 ± 1.7
	D10	1.4 ± 0.2	1.2 ± 0.1	6.8 ± 0.6	4.2 ± 0.3**	13.6 ± 0.2	11.9 ± 0.2**
ρ (mM)	**D0**	0.78 ± 0.04	0.81 ± 0.04	3.30 ± 0.39	3.06 ± 0.47	7.14 ± 0.19	6.44 ± 0.70
	D1	0.70 ± 0.04	0.70 ± 0.19	2.91 ± 0.23	2.87 ± 0.23	5.51 ± 0.08	6.71 ± 0.66
	D10	0.54 ± 0.06	0.47 ± 0.04	2.63 ± 0.22	1.64 ± 0.12**	5.26 ± 0.07	4.62 ± 0.08**